Quantitative reconstructions of annual rainfall in Africa 6000 years ago: Model-data comparison

Odile Peyron,[1] Dominique Jolly,[2] Pascale Braconnot,[3] Raymonde Bonnefille,[4] Joël Guiot,[4] Denis Wirrmann,[5] and Françoise Chalié[4]

Received 12 April 2006; revised 16 June 2006; accepted 28 August 2006; published 23 December 2006.

[1] This paper provides the first set of quantitative reconstructions of annual precipitation for mid-Holocene Africa, based on pollen data. The estimates of precipitation are based on 85 pollen sites ^{14}C dated at 6000 ± 500 years B.P and distributed over the whole of Africa. To improve the reliability of the pollen-based climate reconstruction, two methods are used: the "modern analogues technique" (MAT) and the "plant functional types" (PFT) methods. We then conduct a model-data comparison for five distinct regions, allowing an evaluation of model outputs (the Sahara-Sahel, the eastern Sahara, western equatorial Africa, East Africa, and Madagascar). The pollen-inferred reconstructions are compared with 21 mid-Holocene simulations yielded by Atmospheric General Circulation Models (AGCMs), and coupled ocean-atmosphere-vegetation models (OAVGCMs). The large-scale feature of the hydrological changes is shown to be well captured by most of the models. Data show that during the mid-Holocene, the Sahara was considerably wetter than today (+200 to +700 mm/yr). The results reinforce the conclusion that the AGCMs significantly underestimate this precipitation increase in the Sahara whereas the OAVGCM simulations are in accordance with the data. Our results show that vegetation and ocean feedbacks do not have a strong impact in the intertropical zone and that models fail to properly reproduce the climatic conditions in East Africa and Madagascar. The model-data comparison also suggests that the lengthening of the dry season during boreal winter in the west equatorial region is a robust feature although the pollen-based reconstruction shows no change or only slight drying there.

Citation: Peyron, O., D. Jolly, P. Braconnot, R. Bonnefille, J. Guiot, D. Wirrmann, and F. Chalié (2006), Quantitative reconstructions of annual rainfall in Africa 6000 years ago: Model-data comparison, *J. Geophys. Res.*, *111*, D24110, doi:10.1029/2006JD007396.

1. Introduction

[2] The climate of Africa has varied considerably during the last 20,000 years [*Gasse*, 2000; *Bonnefille and Chalié*, 2000], and during the mid-Holocene period [*deMenocal et al.*, 2000] strong environmental changes occurred in the Sahara. The region was densely vegetated with grasses and shrubs [*Jolly et al.*, 1998a; *Prentice et al.*, 2000], and numerous lakes extended beyond their present level [*Hoelzmann et al.*, 2004]. Paleolake Chad had a surface area of 340,000 km^2 instead of its current 21,000 km^2 [*Servant and Servant-Vildary*, 1980; *Hoelzmann et al.*, 2000], and neolithic civilizations flourished in the Sahara where many elephants, antelopes, giraffes and hippopotami lived [*Petit-Maire et al.*, 1993]. In contrast with the Saharan pattern, the amplitude of the climate changes in west and east equatorial Africa seems almost negligible compared to the present situation [*Elenga et al.*, 2004; *Bonnefille and Chalié*, 2000]. The greening of the Sahara may be explained by the intensification of the African summer monsoon, due to Earth orbital changes. Indeed, experiments with atmospheric general circulation models (AGCMs) show that all models simulate a strengthening of the African monsoon when mid-Holocene insolation is applied as a boundary condition [*COHMAP Members*, 1988; *Joussaume et al.*, 1999; *Braconnot et al.*, 2000a]. However, several studies have reported that vegetation and ocean feedbacks were needed to strengthen the initial signal [*Braconnot et al.*, 2004]. The importance of the feedbacks have been investigated through sensitivity studies which examined the response to changes in (1) land surface [*Texier et al.*, 1997, 2000; *Claussen et al.*, 1999, 2003; *Brostrom et al.*, 1998; *Doherty et al.*, 2000; *De Noblet-Ducoudré et al.*, 2000], (2) desert albedo [*Bonfils et al.*, 2001], and (3) ocean surface [*Kutzbach and Liu*, 1997;

[1]Laboratoire de Chrono-Ecologie, UMR CNRS 6565, Université de Franche-Comté, Besançon, France.
[2]Institut des Sciences de l'Evolution, UMR CNRS 5554, Université Montpellier II, Montpellier, France.
[3]Laboratoire des Sciences du Climat et de l'Environnement/Institut Pierre-Simon Laplace, Unité mixte CEA-CNRS-UVSQ, Gif-sur-Yvette, France.
[4]Centre Européen de Recherche et d'Enseignement des Géosciences de l'Environnement, CNRS UMR 6635, Université Paul Cézanne, Aix-en-Provence, France.
[5]UR055 Paléotropique, Institut de Recherche pour le Développement, Nouméa, New Caledonia.

0148-0227/06/2006JD007396

Hewitt and Mitchell, 1998; *Braconnot et al.*, 2000b, 2004; *Liu et al.*, 2004]. All these experiments showed that, even though the exact location and magnitude of the changes in precipitation at 6000 years B.P. vary substantially from one set of model results to another, land surface and ocean feedbacks significantly increase precipitation in the Sahara. In addition *Braconnot et al.* [1999] showed that ocean feedback further increases the large vegetation feedback in the Sahel regions.

[3] Recent reconstructions of mid-Holocene paleoenvironments focusing on biomes [*Jolly et al.*, 1998a; *Prentice et al.*, 2000] and lake levels [*Kohfeld and Harrison*, 2000] have been used as benchmarks for model evaluation [*Joussaume et al.*, 1999; *Liu et al.*, 2004; *Braconnot et al.*, 2004]. A further step for model-data comparison would be to develop quantitative reconstructions of climate variables based on pollen data, such as those done for Europe [*Cheddadi et al.*, 1997] or East Africa [*Peyron et al.*, 2000]. In this study, we provide the first pollen-based quantitative reconstruction of annual rainfall over the whole of Africa for the mid-Holocene. This data will then serve as a benchmark to evaluate the results of 19 AGCMs and 2 coupled model simulations (OAGCMs) for different regions of Africa. We investigate to determine whether the coupled simulations performed with the IPSL (Institut de Physique Simon Laplace) coupled model taking into account both changes in ocean circulation and in vegetation cover [*Braconnot et al.*, 1999] are in better agreement with data than the atmospheric simulations of the Paleoclimate Modeling Intercomparison Project "PMIP" [*Joussaume et al.*, 1999].

2. Climate Reconstructions and Model Simulations

[4] To improve the reliability of the pollen-inferred paleoclimate reconstruction, two distinct methods are used [*Peyron et al.*, 2000, 2005; *Bonnefille et al.*, 2004]. In the "modern analogues technique" (MAT) method [*Overpeck et al.*, 1985; *Guiot*, 1990], a dissimilarity index calculated between each fossil sample and each modern sample leads to a selection of the ten "best" modern pollen analogues for which the chord distance (i.e., a sum of differences between square root-transformed percentages of the 178 selected taxa) shows the lowest values. The climatic parameter reconstructed value is the weighted average of the climatic parameter at the site of these 10 analogues, according to the inverse distance. The error is defined as the lower and upper extreme climate among these ten analogues. The second method, already tested with success in East Africa [*Peyron et al.*, 2000; *Bonnefille et al.*, 2004] is based on the "plant functional types" (PFT)-climate relationship. Basically, a PFT is defined in terms of functional characteristics (tree/grass, leaf form, phenology) and bioclimatic tolerance. Both methods are based on a modern pollen data set which includes 761 modern pollen samples from Africa and the Arabian Peninsula collected between 17°W and 60°E, 30°N and 33°S at an altitude ranging from 0 to 4000 m [*Jolly et al.*, 1998a]. The 178 pollen taxa identified in the modern data set are each assigned to a PFT, and then for each PFT, a numerical score is calculated following the biomization procedure [*Prentice et al.*, 2000]. The PFT scores derived from modern pollen data are calibrated in terms of climate parameters using an artificial neural network technique [*Caudill and Butler*, 1992; *Peyron et al.*, 1998]. Then, to infer mid-Holocene precipitation values, MAT and PFT methods are applied to the fossil pollen data set including 85 samples from Africa compiled by *Jolly et al.* [1998a].

[5] Our climate reconstructions are used to evaluate model results for five large regions of Africa, where the data coverage is sufficient. The regions includes the Sahara/Sahel, the Intertropical zone (west and east), and Madagascar, over which the precipitation values produced by the model simulations are averaged. For each of these regions, we consider the 19 AGCM simulations of the mid-Holocene climate performed during the first phase of the PMIP (PMIP1 [*Joussaume and Taylor*, 1995]). Since model resolution varies from 1 to 4 degrees in these regions, depending on the model, we designed the regions to include several grid points. Model results were averaged over several seasonal cycles so that error bars for each simulation do not exceed 50 mm/yr. For these PMIP simulations, the Earth's orbital parameters correspond to the values valid for 6000 years ago [*Berger and Loutre*, 1991]. The vegetation and the annual mean cycle of sea surface temperature (SST) are fixed to modern conditions using modern climatology (see http://www-lsce.cea.fr for more information on the experimental protocol). Furthermore, we take into consideration here the OAGCM and the OAVGCM simulations of *Braconnot et al.* [1999] performed with the IPSL model [*Braconnot et al.*, 2000b], so as to test whether ocean and vegetation feedbacks produce results different from the PMIP ones, and whether they are in better agreement with the data. Since AOGCMs are not able to properly reproduce all aspects of the characteristics of modern SST [*Davey et al.*, 2002], the differences in the changes in precipitation simulated with the OAGCM may arise from (1) bias in the simulation of SST for the modern climate and (2) the SST response to the 6ka insolation. To ensure discussion of the impact of the ocean response in our comparisons, we add two additional simulations with the atmospheric component of the coupled model. The first, following the PMIP protocol, is a PMIP simulation for which SST are prescribed to the modern climatology estimated from observations. The second is a PMIP- type simulation for which the SST are prescribed to the SST simulated for the modern climate by the OAGCM. This indicates the impact of the reference SST on the results of the mid-Holocene simulations and also provides information as to how the atmospheric model performs in comparison to the whole of PMIP simulations.

3. Results and Discussion

3.1. Sahara and Sahel

[6] Results indicate that the annual precipitations reconstructed by MAT and PFT methods are similar, showing the same pattern across the Sahara: at 6000 years B.P. (Figures 1 and 2) it was far wetter than today. Figure 3c shows that the chord distances of the modern analogues selected for the 6000 years B.P. climate reconstruction are very low for this area. It implies that these analogues may be considered "very good analogues" to the 6000 years B.P. pollen samples, and thus that the climatic reconstruction is particularly robust for the Sahara-Sahel.

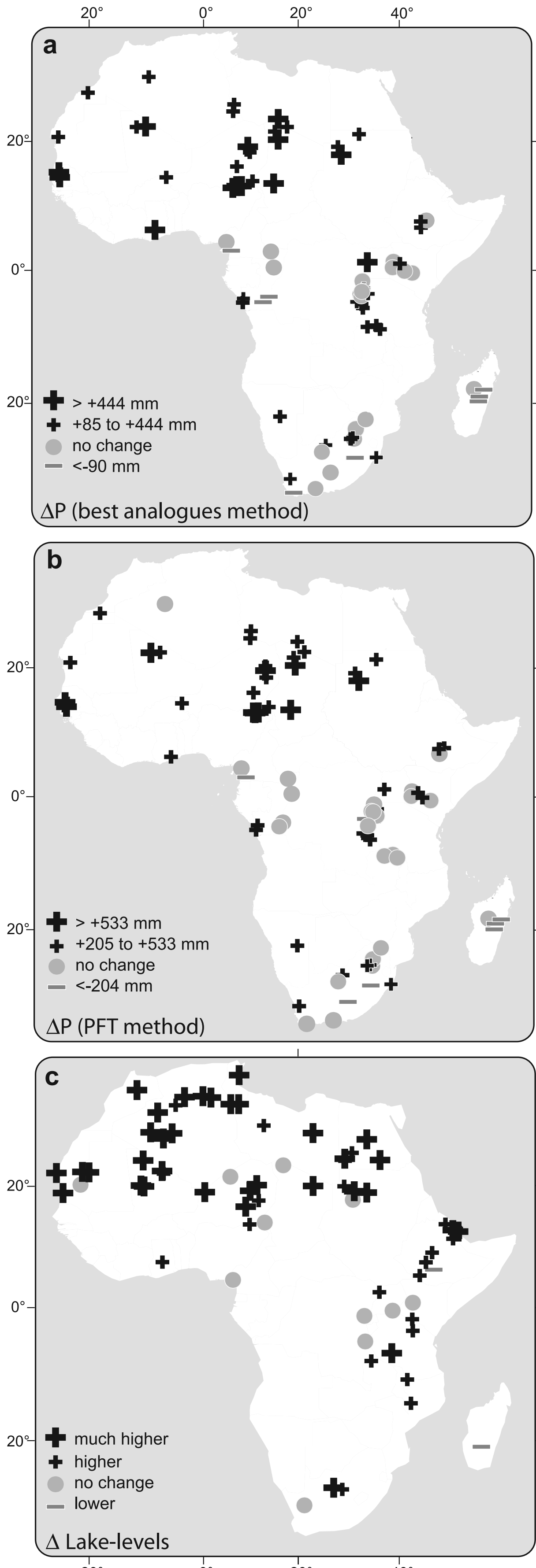

Figure 1. Reconstructed 6000 years B.P. annual precipitation (mm/yr), expressed as anomaly (6000 years B.P. to modern) values, estimated with (a) the MAT and (b) the PFT method. (c) Lake status [*Jolly et al.*, 1998b], expressed as anomaly (6000 years B.P. to modern). For each method the error bars are calculated by applying the method to the modern samples and by plotting the distribution of the observed modern values by classes of predicted values. For each predicted class we calculate the 5th and the 95th percentile providing a 90% confidence interval of the reconstruction. Large changes at 6000 years B.P. are inferred when they are significantly different (at that 90% level) from the modern value, i.e., when the modern value does not belong to the interval. We also consider smaller changes defined by a modern value outside the [25th, 75th] interval because a set of values of low significance may be meaningful simply by mutual coherency.

[7] Between 10 and 30°N, annual precipitation values were greater than now by 85 mm/yr to 500 mm/yr. This is in good agreement with lake status data shown in Figure 1 [*Jolly et al.*, 1998b; *Kohfeld and Harrison*, 2000], and with other sedimentary indicators, archaeological evidence [*Jolly et al.*, 1998a, 1998b; *Street-Perrott and Perrott*, 1993; *Guo et al.*, 2000; *Gasse*, 2000, 2005; *Hoelzmann et al.*, 1998], and stable isotopes studies [*Abell and Hoelzmann*, 2000; *Gasse*, 2002; *Pachur and Hoelzmann*, 2000].

[8] At 6000 years B.P., in western Nubian Paleolake (eastern Sahara, Figure 2) lacustrine carbonates indicate development of a freshwater lake that would require an annual precipitation of 500 to 920 mm/yr [*Hoelzmann et al.*, 2000]. Water balance calculations yielded paleorainfall values of about 460 to 600 mm/yr over the eastern Sahara [*Hoelzmann et al.*, 2001]. For the southeastern Sahara, rainfall estimates based on various and independent indicators such as pollen and other sedimentological data indicate 550 mm/yr [*Kropelin*, 1993], ranging from >300 to 550 mm/yr [*Pachur*, 1991; *Pachur and Hoelzmann*, 1991]. The highest estimate of 700 mm/yr is provided for the crater lake of Mahla [*Mees et al.*, 1991]. Our reconstruction for this region at Oyo (400 to 480 mm/yr), and El Atrun (250 to 950 mm/yr) agrees with the paleorainfall estimates by these authors. The hypothesis of a rainfall dipole within the Sahara is not validated here [*Renssen et al.*, 2006], because no significant longitudinal difference in the magnitude of precipitation anomalies is evidenced (Figure 2).

[9] Figure 2 shows that most PMIP AGCMs produce a 0–100 mm/yr increase in precipitation. Three models have higher rates (100 to 200 mm/yr) and a subset of models suggests a decrease. Previous comparisons of these PMIP simulations have shown that all models produce an increase in precipitation, but that some of them have an east-west pattern with maximum increase further east [*Braconnot et al.*, 2002]. This has been attributed to the way models reproduce the large-scale atmospheric circulation in this region, which also explains some of the differences in atmospheric simulations with interactive vegetation [*De Noblet-Ducoudré et al.*, 2000]. Models with a decrease in precipitation over our western Sahara produce maximum increase either at the coast or further east. In addition, it was shown that models producing

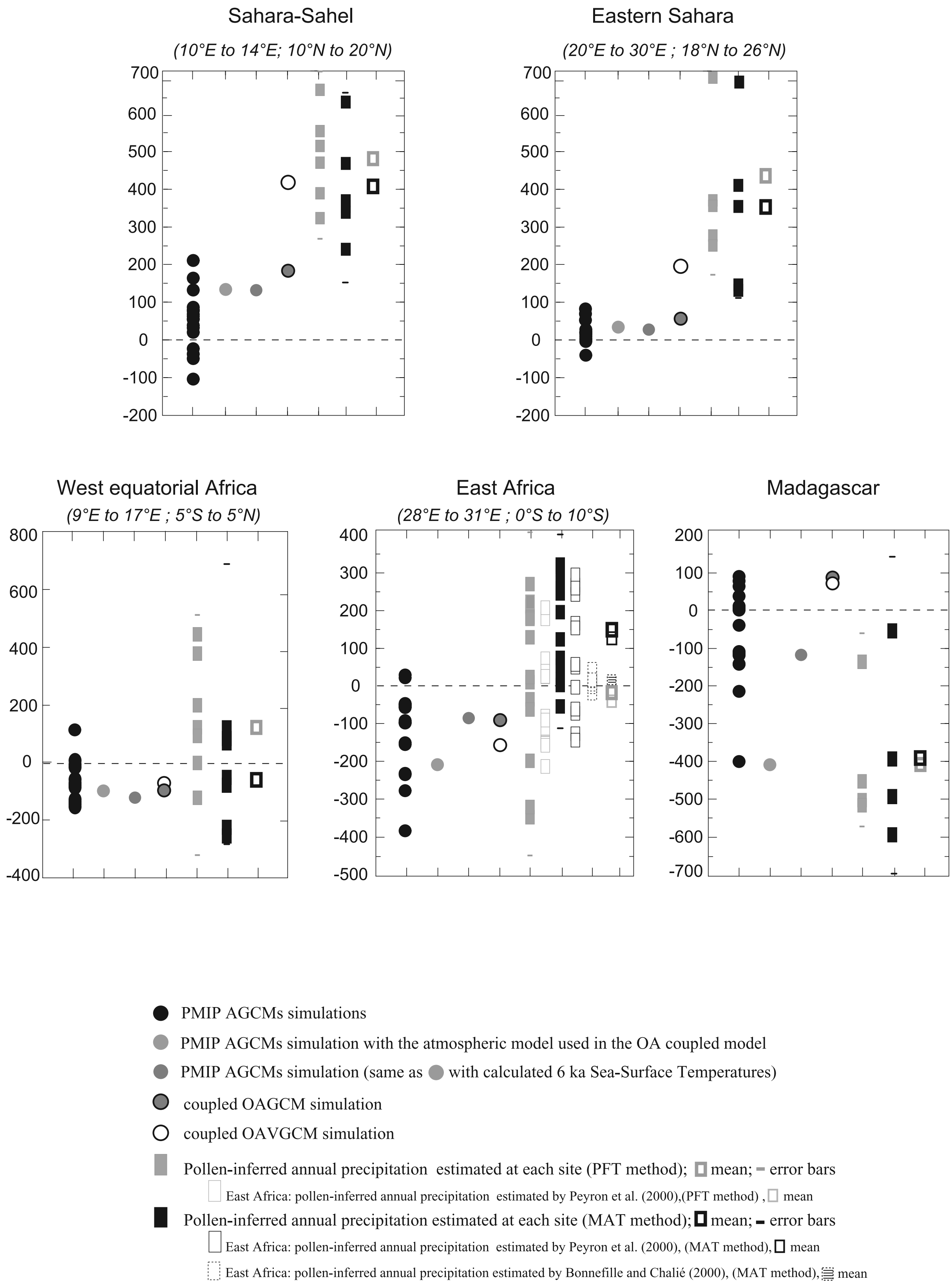
Sahara-Sahel
(10°E to 14°E; 10°N to 20°N)
700
600
500
400
300
200
100
0
-100
-200
Eastern Sahara
(20°E to 30°E ; 18°N to 26°N)
700
600
500
400
300
200
100
0
-100
-200
West equatorial Africa
(9°E to 17°E ; 5°S to 5°N)
800
600
400
200
0
-200
-400
East Africa
(28°E to 31°E ; 0°S to 10°S)
400
300
200
100
0
-100
-200
-300
-400
-500
Madagascar
200
100
0
-100
-200
-300
-400
-500
-600
-700
PMIP AGCMs simulations
PMIP AGCMs simulation with the atmospheric model used in the OA coupled model
PMIP AGCMs simulation (same as with calculated 6 ka Sea-Surface Temperatures)
coupled OAGCM simulation
coupled OAVGCM simulation
Pollen-inferred annual precipitation estimated at each site (PFT method); mean; error bars
East Africa: pollen-inferred annual precipitation estimated by Peyron et al. (2000),(PFT method) , mean
Pollen-inferred annual precipitation estimated at each site (MAT method); mean; error bars
East Africa: pollen-inferred annual precipitation estimated by Peyron et al. (2000), (MAT method), mean
East Africa: pollen-inferred annual precipitation estimated by Bonnefille and Chalié (2000), (MAT method), mean

Figure 2

a modern ITCZ too far north in the simulation of the modern climate also produce precipitation changes further north when compared to the other models. This explains in part why four models produce larger increases in precipitation.

[10] The model-data comparison confirms that all the PMIP simulations consistently underestimate the precipitation increase shown by the data in the Sahara (Figure 2), as found in previous comparisons with pollen or lake data [*Joussaume et al.*, 1999; *Jolly et al.*, 1998b; *Harrison et al.*, 1998; *Coe and Harrison*, 2002]. At 6000 years B.P. the biome distribution shows that steppe vegetation replaces desert as far north as 23°N [*Jolly et al.*, 1998a]. An increase of 200 to 300 mm/yr of precipitation is required for most PMIP models to sustain steppe at 23°N [*Joussaume et al.*, 1999], and here we show that at least an additional amount of 100 to 400 mm/yr of precipitation is required to concur with our reconstruction for this area. This discrepancy underscores the fact that the biome-based estimates of climate change are minimum values only [*Joussaume et al.*, 1999].

[11] The results of the coupled simulations show that although the ocean feedback helps to enhance the African monsoon, only the ocean and vegetation feedbacks produce a precipitation increase in good agreement with the pollen data (Figure 2). The comparison of the two PMIP-type simulations with the atmospheric component of the IPSL model suggests that errors in the simulation of modern SST with the OAGCM do not alter the response of the atmospheric model to insolation forcing. It also shows that this atmospheric model substantially amplifies the monsoon rain compared to other PMIP simulations. The ocean feedback alone only slightly increases the precipitation change. Results including both the vegetation and ocean feedbacks are clearly different from the other simulations and in better agreement with data.

[12] In the eastern Sahara all PMIP simulations produce a precipitation increase of 0–100 mm/yr, which is also insufficient compared to our reconstruction. In this region different SST for the control simulation have no impact on the model results, and ocean feedback marginally increases the precipitation amount. The only simulation that matches the pollen-inferred climatic reconstruction is the one including ocean and vegetation feedbacks. It is also noteworthy that this is the only simulation able to produce an increase both in the eastern and western parts of the Sahelian band.

3.2. Intertropical Zone

[13] The reconstructed climate is comparable to the present one (Figures 1 and 2). However, between 10°N and 20°S, and from west to east the results are more contrasted than in the Sahara.

3.2.1. East Africa

[14] To check the reliability of the reconstruction, the rainfall values estimated here have been compared, in Figure 2, to two spatial climate reconstructions available for East Africa, also based on the MAT and/or the PFT method [*Peyron et al.*, 2000; *Bonnefille and Chalié*, 2000]. These studies show similar climatic patterns in East Africa at 6000 years B.P. It is to be noted that the climate is slightly wetter in the MAT-inferred reconstruction. Nevertheless, *Peyron et al.* [2000] have shown that the results are more spatially homogeneous with the PFT method than with the MAT for East Africa.

[15] Results show that in East Africa, the amplitude of rainfall increase is almost negligible compared to the present situation and in contrast with the Saharan pattern (Figures 1 and 2). This conclusion is in good agreement with previous precipitation estimates inferred from several peat bog sequences in equatorial East Africa [*Bonnefille and Chalié*, 2000; *Chalié*, 1995; *Beuning and Russell*, 2004], and from oxygen isotope data from Mounts Kenya [*Barker et al.*, 2001] and Kilimanjaro [*Thompson et al.*, 2002].

[16] All but two of the PMIP simulations indicate drier conditions in East Africa, from 0 to −400 mm/yr. This pattern may be in agreement with the data located north of 4°S. However, in central southeast Africa, pollen data and high lake levels (Figure 1) indicate unambiguously humid conditions [*Vincens et al.*, 2005] confirmed by the overflow of Lakes Tanganyika, Victoria, Albert and Kivu during the mid-Holocene period [*Gasse*, 2000].

[17] One reason explaining this mismatch between model and data and the wide spread in model results might be the underestimation of the topography in this region, given the spatial resolution of the atmospheric model used here. This underestimation is such that most of the monsoon flow penetrates far to the east over the ocean and is only poorly affected by mountains, or that it produces a local increase in precipitation over high elevations to the north of the equator (not shown). Our results also show that SST of the control simulation has an impact on the simulated change in precipitation, and that the vegetation feedback tends to dry the climate, at least in the model used here. These results suggest that the models do not accurately reproduce east African precipitation and that including ocean and vegetation feedbacks does not improve model performance.

3.2.2. West Africa

[18] In western equatorial Africa, mid-Holocene hydrological conditions reconstructed by the PFT method were similar to or wetter than now, while the MAT-based reconstructions depict the occurrence of similar to or drier conditions than today (Figure 2). To understand such a surprising pattern, and to check whether the discrepancies observed in Figure 2 can be explained by a bias induced by the modern data, we have plotted the actual precipitation values (calculated at each modern pollen site) versus the values inferred from the modern pollen samples belonging to the dominant biomes in West Africa, namely the "tropical seasonal forest" and "tropical rain forest" biomes (Figure 3a). Figure 3a shows that today in West Africa the PFT method under-

Figure 2. Data-model comparison of the mid-Holocene climate for five African key areas. Simulations of annual precipitation based on 19 PMIP models, 1 coupled ocean-atmosphere and 1 coupled ocean-atmosphere-vegetation model [*Braconnot et al.*, 1999] are plotted together with pollen-based annual precipitation estimates (MAT and the PFT methods). Additional simulations with the atmospheric component of the coupled model are shown. The first is a PMIP simulation, and the second is a PMIP-type simulation for which the SST are prescribed to the SST simulated for the modern climate. All results are expressed as anomaly (6000 years B.P. to modern) values. Pollen-based annual precipitation estimated for East Africa with the MAT and/or the PFT methods [*Peyron et al.*, 2000; *Bonnefille and Chalié*, 2000] are also plotted for comparison.

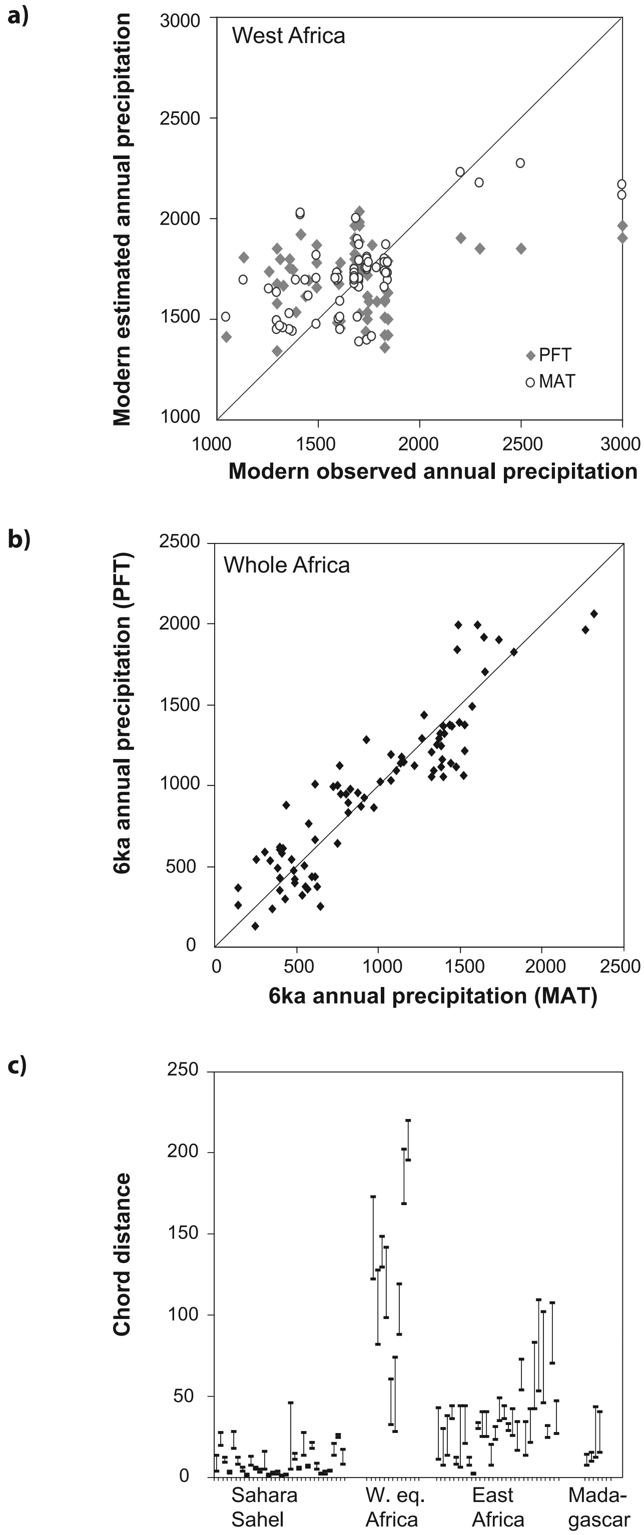

estimates precipitation values above 2000 mm, and that neither method is capable of reproducing modern precipitation around 3000 mm/yr. At 6000 years B.P., the MAT-based spatial reconstruction of the West Africa climate thus seems more reliable. However, our results should be interpreted with caution because they are characterized by deterioration in the quality of the analogues (an increase in chord distance) as well as by numerous ''no-analogue'' situations (Figure 3c). These deviations generally correspond to features of pollen assemblages interpreted in different ways by the two methods. It is also noteworthy that in contrast to west Africa, the scatterplot of the MAT versus PFT precipitation reconstructions for the entire African continent (Figure 3b) demonstrates that the PFT method does not underestimate the magnitude of the precipitation relative to the MAT method for the mid-Holocene period.

[19] *Elenga et al.* [2004] showed that in western equatorial Africa, the greatest extension of dense forest occurred during the interval 10,500–4000 years B.P. However, numerous pollen sequences in west Africa suffer from chronology uncertainties for this time period (bad dating control, low sedimentation rate...). The attribution of the 6000 years B.P. age is then very problematic, except for the well-dated sequence of Lake Barombi Mbo [*Maley and Brenac*, 1998]. Nevertheless, the reconstruction of climatic conditions similar to today's is actually in agreement with the occurrence of the tropical seasonal forests in almost all the sites from western equatorial Africa [*Jolly et al.*, 1998b]. This pattern also agrees with the beginning of sedimentation from 6000 years B.P. in small basins lying in the Guineo-Congolian realm [*Reynaud-Farrera*, 1995], with a low sedimentation rate at Ngamakala in the Congo from 6500 years B.P. [*Elenga et al.*, 1994], and with an SST decrease in the Guinean Gulf between 6500 and 4000 years B.P. [*Morley and Dworetsky*, 1993]. In southwest Cameroon [*Reynaud-Farrera*, 1995; *Giresse et al.*, 2005], like-today conditions are consistent also with low percentages of mature rain forest taxa (Caesalpiniaceae, Sapotaceae) associated with relatively high percentages of *Alchornea* (heliophilous element linked to disturbed rain forest), and Afromontane elements (*Podocarpus* and *Olea capensis*) recognized in Lake Ossa sediments. In the western Cameroon highlands, the lake Bambili record showed that, the precipitation minus evaporation balance was low at 6000 years B.P [*Stager and Anfang-Sutter*, 1999]. For Lake Barombi Mbo, a lower elevation site in western Cameroon, our reconstruction does not show any significant climatic change when compared with today (Figure 1).This result agrees with the lake status inferred by *Talbot et al.* [1984] and

Figure 3. Validation of the pollen-based climatic reconstruction performed on (a) the modern pollen data set. The figure shows, for the modern pollen records belonging to the ''tropical seasonal forest'' and ''tropical rain forest'' equatorial biomes, the pollen-derived annual precipitation (in mm/yr) estimated with the PFT and the MAT methods versus observed precipitation values. (b and c) The 6000 B.P pollen data. Figure 3b is a scatterplot of the MAT versus PFT precipitation reconstruction (in mm/yr) for all sites. In Figure 3c, for the five African key areas, the calculated chord distance of the closer and the less close of the 10 best modern analogues selected by the MAT is plotted.

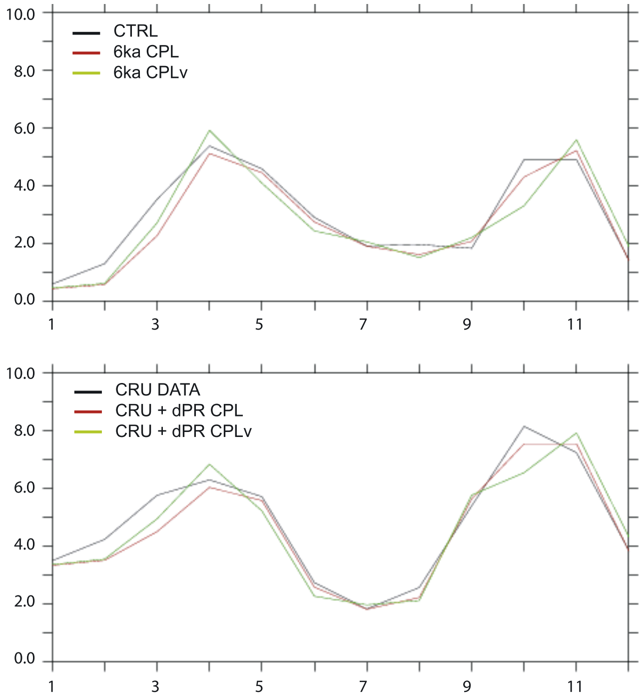

Figure 4. Monthly rainfall distribution (mm/month) in western Africa [9°E to 17°E, 5°S to 5°N]: (a) simulated for the control experiment (CTRL), 6 kyr coupled OAGCM simulation (CPL), and 6 kyr coupled OAVGCM simulation (CPLv) and (b) CRU present climatology (CRU data), CRU climatology plus anomalies between 6 kyr OAGCM and control (CRU+ dPR CPL), and CRU climatology plus anomalies between 6 kyr OAVGCM and control (CRU + dPR CPLv).

with the observed low frequencies of the main taxa of the Biafran evergreen forest at 6000 years B.P. [*Maley and Brenac*, 1998].

[20] The contradiction between the MAT and PFT results certainly deserves more investigation. Additional modern samples will be required from equatorial Africa to improve the reconstruction of the complex climatic conditions occurring during this period.

[21] A previous model-data comparison [*Jolly et al.*, 1998b] has concluded that the model simulation at 6000 years B.P. was not reliable in central Africa because simulated annual precipitation values were 300 mm/yr lower than the modern ones over Cameroon, Gabon, and the Congo. Here, all PMIP simulations show that annual precipitation was lower than today by 0–200 mm/yr (Figure 2). Furthermore, the OAGCM and OAVGCM simulations show similar results, suggesting that the precipitations of this region are only poorly affected by the ocean and vegetation feedbacks. The whole response is thus dominated by the response of atmospheric circulation to insolation forcing.

[22] A more detailed analysis of the model results suggests that it appears reasonable to find no change or a slight drying in this region. The climate of the tropical zone is governed by the seasonal movement of the Intertropical Convergence Zone (ITCZ) in response to changes in the location of maximum solar heating. Lower rainfall in West Africa may be due to the extent of the ITCZ migration northward during the northern hemisphere summer and southward during the corresponding winter. This hypothesis might imply that the ITCZ will not be blocked for some months within the intertropical area like today. This should lead to a longer dry season in winter or/and in summer.

[23] This hypothesis of a longer dry season in winter or/and in summer is confirmed by the results of the IPSL 6ka AOGCM and 6 ka AOVGCM experiments (Figure 4a). Seasonal rainfall distribution within the year averaged from 9°E to 17°E and 5°S to 5°N, shows that both the winter and summer dry season terminate almost one month later at 6ka than today in the two coupled simulations. We know that the control simulation is too dry during the winter dry season and we correct this bias by adding the simulated anomalies (6 ka minus control) to the CRU (Climatic Research Unit) modern climatology [*Hulme*, 1992]. Figure 4b shows that this correction has no impact on the lengthening of the winter dry season while the summer dry season is not really changed. The budget of these changes over the year is a small change of about 100 mm/yr, in agreement with the MAT reconstruction. The change in rainfall seasonality in western equatorial Africa thus appears to be a good benchmark for model-data comparison. Statistical reconstruction of this seasonality from pollen data is difficult and will require the use of a vegetation model to test the effect of changes in dry season length versus changes in annual precipitation.

3.3. Madagascar

[24] Between 10 and 20°S, there is a complete lack of available pollen data on the continent, but drier conditions are also found for Madagascar (annual precipitation mean around −400 mm/yr). This result concurs with the relatively dry conditions suggested at Tritrivakely (~20°S) by multiproxy paleoenvironmental reconstructions [*Williamson et al.*, 1998; *Gasse and van Campo*, 1998]. Furthermore, Figure 3c shows that the climatic reconstruction for Madagascar can be considered reliable because the chord distances of the modern analogues selected are very low for this area.

[25] Here, most PMIP simulations match our reconstruction well, although several PMIP simulations produce a 0 to 100 mm/yr precipitation increase (Figure 2). Results with the IPSL model suggest that the coupled OAGCM has trouble reproducing both the modern SST conditions and the way SST changes at 6000 years B.P. in this region. Indeed, the addition of the different feedbacks deteriorates the model results in this region strongly influenced by oceanic conditions. It is not clear why ocean and vegetation feedbacks would worsen the fit to the data; this requires further investigation.

4. Summary and Conclusions

[26] This study provides the first quantitative pollen-based reconstruction of precipitation for all of Africa at 6000 years B.P., compared with outputs of AGCMs and coupled ocean-atmosphere-vegetation models. Pollen data show that Saharan precipitation was 200–700 mm/yr greater than at present, versus the 200–300 mm/yr estimate based upon biome-scale shifts in the vegetation. The model-data comparison demonstrates that the inclusion of vegetation feedbacks in a coupled ocean-atmosphere-vegetation model considerably improves the data-model matches for the

Sahara. In contrast to previous studies, this analysis also took other regions of Africa into account. Our results show that the models considered here fail to properly represent the changes in precipitation in eastern equatorial Africa. Results with the IPSL model where ocean and vegetation feedback are introduced show that these feedbacks are not well reproduced in eastern equatorial Africa or Madagascar. A poor representation of the topography in East Africa and the difficulties in properly simulating SST in the Indian Ocean may be the cause of these model drawbacks. In western equatorial Africa, the apparent contradiction between the results inferred by the MAT and the PFT methods certainly deserves further investigation so as to improve the reconstruction of complex climatic conditions occurring during this period. However, model results show that the lengthening of the dry season during the boreal winter in the west equatorial region seems to be a robust feature across model simulations. It is attributed to the fact that the ITCZ is located further north compared to modern conditions during boreal summer and further south during boreal winter. Thus the time spent by the ITCZ in west equatorial Africa is reduced, thereby increasing the length of the dry season.

[27] Our paleoclimatic data set can now be used to evaluate further model simulations on the scale of the entire African continent. It is crucial to provide such climatic information in several regions of Africa to be able to evaluate the consistency of the simulated climate, not only its local features, but also its potential longitudinal and latitudinal gradients or contrasts. Although the spatial distribution of the data needs to be improved, particularly in the intertropical region, this data set will be used, in the future, to fully test coupled model simulations (PMIP2) and help to better infer the role of the ocean and vegetation feedbacks on this continent. This will be completely achieved by a better evaluation of data, as well as model simulations, in particular concerning the monthly distribution of precipitation.

[28] **Acknowledgments.** Financial support was provided by the European Union through the MOTIF project (EVK2-CT-2002-00153) and by the French (INSU/CNRS) PNEDC through the ECHO project. This work is a contribution to PMIP, IGBP GAIM/GCTE/PAGES/BIOME 6000. The authors express their sincere thanks to John Olsen for his help with the English language, and ollen contributors: A. Ballouche, P. Brénac, G. Buchet, D. Burney, R. Cheddadi, A.C. Hamilton, H. Elenga, H. Lamb, A.M. Lézine, J. Maley, M. Reille, G. Riollet, L. Scott, I. Ssemmanda, H. Straka, D. Taylor, M. Umer, E. Van Campo, A. Vincens, and M. Waller.

References

Abell, P., and P. Hoelzmann (2000), Holocene palaeoclimates in northwestern Sudan: Stable isotope studies on molluscs, *Global Planet. Change*, *26*, 1–12.

Barker, P. A., F. A. Street-Perrott, M. J. Leng, P. B. Greenwood, D. L. Swain, R. A. Perrott, R. J. Telford, and K. J. Ficken (2001), A 14,000-year oxygen isotope record from diatom silica in two alpine lakes on Mt. Kenya, *Science*, *292*, 2307–2310.

Berger, A., and M. F. Loutre (1991), Insolation values for the climate of the last 10 million years, *Quat. Sci. Rev.*, *10*, 297–317.

Beuning, K. R. M., and J. M. Russell (2004), Vegetation and sedimentation in the Lake Edward Basin, Uganda-Congo during the late Pleistocene and early Holocene, *J. Paleolimnol.*, *32*, 1–18.

Bonfils, C., N. de Noblet-Ducoudré, P. Braconnot, and S. Joussaume (2001), Hot desert albedo and climate change: Mid-Holocene monsoon in north Africa, *J. Clim.*, *14*, 3724–3737.

Bonnefille, R., and F. Chalié (2000), Pollen-inferred precipitation time-series from equatorial mountains, Africa, the last 40 kyr B.P., *Global Planet. Change*, *26*, 25–50.

Bonnefille, R., R. Potts, F. Chalié, D. Jolly, and O. Peyron (2004), High-resolution vegetation and climate change associated with Pliocene Australopithecus afarensis, *Proc. Natl. Acad. Sci. U. S. A.*, *101*, 12,125–12,129.

Braconnot, P., S. Joussaume, O. Marti, and N. de Noblet (1999), Synergistic feedbacks from ocean and vegetation on the African monsoon response to mid-Holocene insolation, *Geophys. Res. Lett.*, *26*, 2481–2484.

Braconnot, P., S. Joussaume, N. de Noblet, and G. Ramstein (2000a), Mid-Holocene and Last Glacial Maximum African monsoon changes as simulated within the Paleoclimate Modelling Intercomparison Project, *Global Planet. Change*, *26*, 51–66.

Braconnot, P., O. Marti, S. Joussaume, and Y. Leclainche (2000b), Ocean feedback in response to 6 kyr B.P. insolation, *J. Clim.*, *13*, 1537–1553.

Braconnot, P., M. F. Loutre, B. Dong, S. Joussaume, and P. Valdes (2002), How the simulated change in monsoon at 6 ka B.P. is related to the simulation of the modern climate: Results from the Paleoclimate Modeling Intercomparison Project, *Clim. Dyn.*, *19*, 107–121.

Braconnot, P., S. P. Harrison, S. Joussaume, C. D. Hewitt, A. Kitoh, J. E. Kutzbach, Z. Liu, B. Otto-Bliesner, J. Syktus, and N. Weber (2004), Evaluation of PMIP coupled ocean-atmosphere simulations of the mid-Holocene, in *Past Climate Variability Through Europe and Africa*, edited by R. W. Battarbee, F. Gasse, and C. E. Stickley, pp. 515–533, Springer, New York.

Brostrom, A., M. Coe, S. P. Harrison, R. Gallimore, J. E. Kutzbach, J. Foley, I. C. Prentice, and P. Behling (1998), Land surface feedbacks and palaeomonsoons in northern Africa, *Geophys. Res. Lett.*, *25*, 3615–3618.

Caudill, M., and C. Butler (1992), *Understanding Neural Networks 1, Basic Networks*, MIT Press, Cambridge, Mass.

Chalié, F. (1995), Paléoclimats du bassin Tanganyika Sud au cours des 25 derniers mille ans: reconstitution quantitative par le traitement statistique des données polliniques, *C. R. Acad. Sci. Ser. 2a Sci. Terre Planetes*, *320*, 205–210.

Cheddadi, R., G. Yu, J. Guiot, S. P. Harrison, and I. C. Prentice (1997), The climate of Europe 6000 years ago, *Clim. Dyn.*, *13*(1), 1–9.

Claussen, M., C. Kubatzki, V. Brovkin, A. Ganopolski, P. Hoelzmann, and H. J. Pachur (1999), Simulation of an abrupt change in Saharan vegetation in the mid-Holocene, *Geophys. Res. Lett.*, *26*, 2037–2040.

Claussen, M., V. Brovkin, A. Ganopolski, C. Kubatzki, and V. Petoukhov (2003), Climate change in northern Africa: The past is not the future, *Clim. Change*, *57*(1), 99–118.

Coe, M. T., and S. P. Harrison (2002), The water balance of northern Africa during the mid-Holocene: An evaluation of the 6 ka B.P. PMIP simulations, *Clim. Dyn.*, *19*, 155–166.

COHMAP Members (1988), Climatic changes of the last 18,000 years: Observations and model simulations, *Science*, *241*, 1043–1052.

Davey, M. K., et al. (2002), STOIC: A study of coupled model climatology and variability in tropical ocean regions, *Clim. Dyn.*, *18*, 403–420.

deMenocal, P., J. Ortiz, T. Guilderson, J. Adkins, M. Sarnthein, L. Baker, and M. Yarusinsky (2000), Abrupt onset and termination of the African Humid Period: Rapid climate responses to gradual insolation forcing, *Quat. Sci. Rev.*, *19*, 347–361.

De Noblet-Ducoudré, N., M. Claussen, and I. C. Prentice (2000), Mid-Holocene greening of the Sahara: First results of the GAIM 6000 year B.P. experiment with two asynchronously coupled atmosphere/biome models, *Clim. Dyn.*, *16*, 643–659.

Doherty, R., J. Kutzbach, J. Foley, and D. Pollard (2000), Fully coupled climate/dynamical vegetation model simulations over northern Africa during the mid-Holocene, *Clim. Dyn.*, *16*, 561–573.

Elenga, H., D. Schwartz, and A. Vincens (1994), Pollen evidence of late Quaternary vegetation and inferred climate changes in Congo, *Palaeogeogr. Palaeoclimatol. Palaeoecol.*, *109*, 345–356.

Elenga, H., J. Maley, A. Vincens, and I. Farrera (2004), Palaeoenvironnments, palaeoclimates and landscapes development in Atlantic equatorial Africa: A review of key sites covering the last 25 kyrs, in *Past Climate Variability Through Europe and Africa*, edited by R. W. Battarbee, F. Gasse, and C. E. Stickley, pp. 181–198, Springer, New York.

Gasse, F. (2000), Hydrological changes in the African tropics since the last glacial maximum, *Quat. Sci. Rev.*, *19*, 189–211.

Gasse, F. (2002), Diatom-inferred salinity and carbonate oxygen isotopes in Holocene waterbodies of the western Sahara and Sahel (Africa), *Quat. Sci. Rev.*, *21*, 737–767.

Gasse, F. (2005), Continental palaeohydrology and palaeoclimate during the Holocene, *C. R. Geosci.*, *337*, 79–86.

Gasse, F., and E. van Campo (1998), A 40,000-yr pollen and diatom record from Lake Tritrivakely, Madagascar, in the southern tropics, *Quat. Res.*, *49*, 299–311.

Giresse, P., J. Maley, and A. Kossoni (2005), Sedimentary environmental changes and millennial climatic variability in a tropical shallow lake (Lake Ossa, Cameroon) during the Holocene, *Palaeogeogr. Palaeoclimatol. Palaeoecol.*, *218*, 257–285.

Guiot, J. (1990), Methodology of palaeoclimatic reconstruction from pollen in France, *Palaeogeogr. Palaeoclimatol. Palaeoecol.*, *80*, 49–69.

Guo, Z., N. Petit-Maire, and S. Kröpelin (2000), Holocene non-orbital climatic events in present-day arid areas of northern Africa and China, *Global Planet. Change*, *26*, 97–103.

Harrison, S. P., et al. (1998), Intercomparison of simulated global vegetation distributions in response to 6 kyr B.P. orbital forcing, *J. Clim.*, *11*, 2721–2742.

Hewitt, C. D., and J. F. B. Mitchell (1998), A fully coupled GCM simulation of the climate of the mid-Holocene, *Geophys. Res. Lett.*, *25*, 361–364.

Hoelzmann, P., D. Jolly, S. P. Harrison, F. Laarif, R. Bonnefille, and H. J. Pachur (1998), Mid-Holocene land-surface conditions in northern Africa and the Arabian peninsula: A data set for the analysis of biogeophysical feedbacks in the climate system, *Global Biochem. Cycles*, *12*, 35–52.

Hoelzmann, P., H. J. Kruse, and F. Rottinger (2000), Precipitation estimates for the eastern Saharan palaeomonsoon based on a water balance model of the West Nubian palaeolake basin, *Global Planet. Change*, *26*, 105–120.

Hoelzmann, P., B. Keding, H. Berke, S. Kröpelin, and H. J. Kruse (2001), Environmental change and archaeology: Lake evolution and human occupation in the eastern Sahara during the Holocene, *Palaeogeogr. Palaeoclimatol. Palaeoecol.*, *169*, 193–217.

Hoelzmann, P., F. Gasse, L. Dupont, U. Salzmann, M. Staubwasser, D. Leuschner, and F. Sirocko (2004), Palaeoenvironmental changes in the arid and subarid belt (Sahara-Sahel-Arabian peninsula) from 150 kyr to present, in Past Climate Variability through Europe and Africa, R. W. Battarbee, F. Gasse, and C. E. Stickley, pp. 219–256, Springer, New York.

Hulme, M. (1992), A 1951–80 global land precipitation climatology for the evaluation of General Circulation Models, *Clim. Dyn.*, *7*, 57–72.

Jolly, D., et al. (1998a), Biome reconstruction from pollen and plant macrofossil data for Africa and the Arabian peninsula at 0 and 6000 years, *J. Biogeogr.*, *25*, 1007–1027.

Jolly, D., S. P. Harrison, B. Damnati, and R. Bonnefille (1998b), Simulated climate and biomes of Africa during the late Quaternary: comparison with pollen and lake status data, *Quat. Sci. Rev.*, *17*, 629–657.

Joussaume, S., and K. E. Taylor (1995), Status of the Paleoclimate Modeling Intercomparison Project (PMIP), *WCRP-92*, *WMO/TD 732*, pp. 425–430, World Clim. Res. Programme, Geneva, Switzerland.

Joussaume, S., et al. (1999), Monsoon changes for 6000 years ago: Results of 18 simulations from the Paleoclimate Modeling Intercomparison Project (PMIP), *Geophys. Res. Lett.*, *26*, 859–862.

Kohfeld, K. E., and S. P. Harrison (2000), How well can we simulate past climates? Evaluating the models using global palaeoenvironmental datasets, *Quat. Sci. Rev.*, *19*, 321–346.

Kropelin, S. (1993), Zur Rekonstruktion der spätquartären Umwelt am Unteren Wadi Howar Südöstliche Sahara/NW Sudan, *Berl. Geogr. Abh.*, *54*, 1–293.

Kutzbach, J. E., and Z. Liu (1997), Response of the African monsoon to orbital forcing and ocean feedbacks in the middle Holocene, *Science*, *278*, 440–443.

Liu, Z., S. P. Harrison, J. E. Kutzbach, and B. Otto-Bliesner (2004), Global monsoons in the mid-Holocene and oceanic feedback, *Clim. Dyn.*, *22*, 157–182.

Maley, J., and P. Brenac (1998), Vegetation dynamics, palaeoenvironments and climatic changes in the forests of western Cameroon during the last 28,000 years B.P., *Rev. Palaeobot. Palynol.*, *99*, 157–187.

Mees, F., R. Nijs, and H. Dumont (1991), Holocene evolution of the crater lake at Malha, northwestern Sudan, *J. Paleolimnol.*, *5*, 227–253.

Morley, J. J., and B. A. Dworetsky (1993), Holocene temperature patterns in the South Atlantic, Southern, and Pacific oceans, in *Global Climates Since the Last Glacial Maximum*, edited by H. E. Wright et al., pp. 125–135, Univ. of Minn. Press, Minneapolis.

Overpeck, J. T., T. Webb III, and I. C. Prentice (1985), Quantitative interpretation of fossil pollen spectra: Dissimilarity coefficients and the method of modern analogs, *Quat. Res.*, *23*, 87–108.

Pachur, H.-J. (1991), Tethering stones as palaeoenvironmental indicators, *Sahara*, *4*, 13–32.

Pachur, H.-J., and P. Hoelzmann (1991), Paleoclimatic implications of late Quaternary lacustrine sediments in Western Nubia, Sudan, *Quat. Res.*, *36*, 257–276.

Pachur, H.-J., and P. Hoelzmann (2000), Late Quaternary palaeoecology and palaeoclimates of the eastern Sahara, *J. Afr. Earth Sci.*, *30*, 929–939.

Petit-Maire, N., N. Page, and J. Marchand (1993), The Sahara in the Holocene, map 1/5.000.000, U. N. Educ., Sci. and Cult. Organ./Comm. for the Geol. Map of the World, Paris, France.

Peyron, O., J. Guiot, R. Cheddadi, P. E. Tarasov, M. Reille, J. L. de Beaulieu, S. Bottema, and V. Andrieu (1998), Climatic reconstruction in Europe for 18,000 yr B.P. from pollen data, *Quat. Res.*, *49*, 183–196.

Peyron, O., D. Jolly, R. Bonnefille, A. Vincens, and J. Guiot (2000), Climate of East Africa 6000 ^{14}C yr B.P., as inferred from pollen data, *Quat. Res.*, *54*, 90–101.

Peyron, O., C. Bégeot, S. Brewer, O. Heiri, M. Magny, L. Millet, P. Ruffaldi, E. Van Campo, and G. Yu (2005), Late glacial climatic changes in eastern France (Lake Lautrey) from pollen, lake-levels, and chironomids, *Quat. Res.*, *64*, 197–211.

Prentice, I. C., D. Jolly, and BIOME 6000 Participants (2000), Mid-Holocene and glacial-maximum vegetation geography of the northern continents and Africa, *J. Biogeogr.*, *27*, 507–519.

Renssen, H., V. Brovkin, T. Fichefet, and H. Goosse (2006), Simulation of the Holocene climate evolution in northern Africa: The termination of the African Humid Period, *Quat. Int.*, *150*, 95–102.

Reynaud-Farrera, I. (1995), Histoire des paléoenvironnements forestiers du Sud-Cameroun à partir d'analyses palynologiques et statistiques de dépôts holocènes et actuels, Ph.D. thesis, 198 pp., Univ. Montpellier 2, Montpellier, France.

Servant, M., and S. Servant-Vildary (1980), L'environnement quaternaire du bassin du Tchad, in *The Sahara and the Nile*, edited by M. A. J. Williams and H. Faure, pp. 133–162, A. A. Balkema, Brookfield, Vt.

Stager, J. C., and R. Anfang-Sutter (1999), Preliminary evidence of environmental changes at Lake Bambili (Cameroon, West Africa) since 24,000 B.P., *J. Paleolimnol.*, *22*, 319–330.

Street-Perrott, F. A., and R. A. Perrott (1993), Holocene vegetation, lake levels and climate of Africa, in *Global Climates Since the Last Glacial Maximum*, edited by H. E. Wright et al., pp. 318–356, Univ. of Minn. Press, Minneapolis.

Talbot, M. R., D. A. Livingstone, P. G. Palmer, J. Maley, J. M. Melack, G. Delibrias, and S. Gulliksen (1984), Preliminary results from sediment cores from Lake Bosumtwi, Ghana, in *Palaeoecology of Africa and the Surrounding Islands*, vol. 16, edited by J. A. Coetzee and E. M. Van Zinderen Bakker, pp. 173–192, A. A. Balkema, Brookfield, Vt.

Texier, D., N. de Noblet, S. P. Harrison, A. Haxeltine, D. Jolly, S. Joussaume, F. Laarif, I. C. Prentice, and P. Tarasov (1997), Quantifying the role of biosphere-atmosphere feedbacks in climate change: coupled model simulation for 6000 years B.P. and comparison with palaeodata for northern Eurasia and northern Africa, *Clim. Dyn.*, *13*, 865–882.

Texier, D., N. de Noblet, and P. Braconnot (2000), Sensitivity of the African and Asian monsoons to mid-Holocene insolation and data-inferred surface changes, *J. Clim.*, *13*, 164–181.

Thompson, L. G., et al. (2002), Kilimanjaro ice core records: Evidence of Holocene climate change in tropical Africa, *Science*, *298*, 589–593.

Vincens, A., G. Buchet, D. Williamson, and M. Taieb (2005), A 23,000 yr pollen record from Lake Rukwa (8°S, SW Tanzania): New data on vegetation dynamics and climate in central eastern Africa, *Rev. Palaeobot. Palynol.*, *137*, 147–162.

Williamson, D., A. Jelinowska, C. Kissel, P. Tucholka, E. Gibert, F. Gasse, M. Massault, M. Taieb, E. Van Campo, and K. Wiekowski (1998), Mineral-magnetic proxies of erosion/oxidation cycles in tropical maar-lake sediments (Lake Tritrivakely, Madagascar): Paleoenvironmental implications, *Earth Planet. Sci. Lett.*, *155*, 205–219.

R. Bonnefille, F. Chalié, and J. Guiot, Centre Européen de Recherche et d'Enseignement des Géosciences de l'Environnement, CNRS UMR 6635, Université Paul Cézanne, BP 80, F-13545 Aix-en-Provence cedex 04, France. (bonnefille@cerege.fr; guiot@cerege.fr; guiot@cerege.fr)

P. Braconnot, Laboratoire des Sciences du Climat et de l'Environnement/Institut Pierre-Simon Laplace, Unité mixte CEA-CNRS-UVSQ, F-91191 Gif-sur-Yvette Cedex, France. (pascale.braconnot@cea.fr)

D. Jolly, Institut des Sciences de l'Evolution, Case 61, UMR CNRS 5554, Université Montpellier II, F-34095 Montpellier cedex 5, France. (jolly@isem.univ-montp2.fr)

O. Peyron, Laboratoire de Chrono-Ecologie, UMR CNRS 6565, Université de Franche-Comté, F-25030 Besançon, France. (odile.peyron@univ-fcomte.fr)

D. Wirrmann, UR055 Paléotropique, Institut de Recherche pour le Développement, BP A5, F-98848 Nouméa cedex, New Caledonia. (denis.wirrmann@noumea.ird.nc)